Journal of Alloys and Compounds, 211/212 (1994) 83–89
JALCOM 081

Amplitude-dependent internal friction and plasticity of crystals*

B.K. Kardashev, S.B. Kustov, A.B. Lebedev and S.P. Nikanorov
A.F. Ioffe Physico-Technical Institute, Russian Academy of Sciences, St. Petersburg 194021 (Russian Federation)

Abstract

The effects of temperature, prestrain and *in situ* plastic deformation on the amplitude dependences of the internal friction and Young's modulus defect were studied on a number of alkali halides and metals at a frequency of about 10^5 Hz. In order to study the effect of the frequency the amplitude dependence of internal friction and Young's modulus defect were investigated at 10^{-3}–10 Hz. The correlation between micro- and macroplasticity is discussed. These results are considered phenomenologically on the basis of the assumption that dislocations overcome long- and short-range obstacles by means of force and thermofluctuation mechanisms.

1. Introduction

The amplitude-dependent internal friction (ADIF) and Young's modulus defect (YMD) of crystals are determined by the hysteresis of the dislocation displacement under vibrational stress. Therefore the investigation of ADIF can give information about the dislocation dynamics and plastic deformation. This information is valuable particularly because it can be obtained by measurements at very low stress levels. The aim of the series of investigations reviewed here was to elucidate the effect of different factors on the ADIF and YMD (temperature, frequency, plastic deformation, different structure and character of the interatomic forces, impurity concentration). The investigations were performed using various experimental techniques.

2. Experimental techniques and materials

The amplitude dependences of the logarithmic decrement δ and YMD $\Delta E/E$ were investigated using a composite resonator [1] for longitudinal vibrations, at frequencies near 10^5 Hz and strain amplitudes of 10^{-7}–10^{-4}. Prestrained single crystals with the NaCl structure (NaCl [2, 3], NaF [2, 4, 5], LiF [2, 6, 7] and MgO [8], some of them with different impurity contents [2, 5–7]), with an f.c.c. lattice (Al and Al-based alloys [2, 9, 10]), and with a b.c.c. lattice (Mo) [11] were investigated. Besides, trigonal Bi crystals were studied for different crystallographic orientations [2, 12].

Simultaneous measurements of decrement and external load, giving the plastic deformation, were made. A rod-shaped specimen was deformed by three-point bending. The load was applied at the nodes of a standing wave [2, 13]. The crystals of NaCl type [13–15], with an f.c.c. [16] and an h.c.p. [17] lattice were studied by this technique. All the experiments were performed with the help of a computer-controlled set-up [16] in order to provide the necessary rate of ADIF measurements.

Measurements of ADIF and YMD at frequencies of (5×10^{-3}–5 Hz and strain amplitudes of 10^{-6}–3×10^{-5}) were carried out by computer-controlled registration of stress–strain hysteresis loops [18]. The load was measured by the tensometric gauge of an Instron device, and the compression strain by a capacity gauge with a resolution of about 10^{-8}. These low frequency investigations were performed on prestrained LiF and NaCl [18–21], Al and Zn [22] single crystals.

3. ADIF in the ultrasonic range

Investigations of ADIF and YMD of predeformed crystals revealed the following regularities. Preliminary plastic deformation causes the amplitude dependence of δ and $\Delta E/E$. The ADIF and YMD decrease smoothly with decreasing temperature. The ADIF is approximately equal to the YMD and is given by a power function of the strain amplitude ϵ_0:

$$\delta_h = r(\Delta E/E) = A\epsilon_0^n$$

Here $r \approx 1$, and n is a numerical factor typical for the specific material and depends on postdeformation ageing, impurity content and dose of X-ray irradiation, but not on temperature.

*Invited paper.

SSDI 0925-8388(93)00081-9

The above-mentioned regularities were observed in all the crystals studied, excluding the trigonal Bi crystal [2, 12]. Bi single crystals were regarded as pseudo-f.c.c. crystals. It was shown that ADIF is a power function of ϵ_0 as for the other crystals for the orientations where the easy glide system $\{111\}\langle 110\rangle$ is active. In this case dislocations oscillate in the field of mainly central forces of Van der Waals type and partly metallic in nature. For other orientations when the secondary glide system and the $\{110\}\langle 001\rangle$ system of twinning are active, dislocation motion takes place in the field of covalent binding forces. The amplitude dependences of IF have a power form $\delta_h \alpha \epsilon_0^n$ where $n=f(T)$. The change of the mechanism of damping was attributed to the alteration of the glide systems [2].

In some crystals (LiF, Al) hysteresis in $\delta_h(\epsilon_0)$ and a change in δ_h with time were observed. These effects were ascribed to the mobility of point defects or reorientation of anisotropic centres pinning dislocations [2, 6].

The ADIF and YMD are often considered in the framework of the string models of the breakaway of dislocations from pinning point defects [23–26]. The revealed regularities in the behaviour of the ADIF and YMD with the change of various factors were claimed in refs. 2, 27 and 28 not to contradict the theory of thermally activated breakaway of double-dislocation segments by Indenbom and Chernov [24]. According to the theory the functional form of $\delta_h(\epsilon_0)$ is set by the dislocation segment length distribution function. It was suggested that from the dependences $\delta_h(\epsilon_0)$ at different T values the stress amplitude $\tau_\delta(T)$ could be found at a constant δ_h which corresponds to the breakaway of segments with lengths longer than $L_h=F/b\tau$. Here F is the binding force, and b is the Burgers vector. This dependence $\tau_\delta(T)$ gives the possibility of extracting the dependence of the activation length d on the binding force. The inverse dependence $F(d)$ was determined by Schwarz and Granato [25] as the profile of the dislocation–point defect interaction force law. Examples of such analysis can be found in refs. 2, 5–7, 9 and 27–29. However, further investigations [10, 11, 30] showed that the algorithm proposed in ref. 24 failed to give finite values of the binding energy H_0 between a dislocation and a point defect. It was supposed that the ADIF reflects a more complex phenomenon than interaction of single dislocation loops with pinning points.

Schwarz and Granato [25] suggested considering the stress amplitude τ_δ as a microscopic yield stress. It was found [5, 27] that the temperature dependence of τ_δ for alkali halides (NaF, NaF:Ca^{2+}, NaCl) correlates with the temperature dependence of the yield stress $\tau_s(T)$. Such a correlation was observed in copper alloy [31] and aluminium [9].

The temperature dependences of τ_δ and τ_s for NaF and LiF are shown in Fig. 1 and for Al in Fig. 2. The dependences $\tau_\delta(T)$ were so plotted as to agree with $\tau_s(T)$ at approximately 100 K. A correlation between the dependences of τ_δ and τ_s on the impurity concentration for LiF:Mg^{2+} and NaF:Ca^{2+} was also observed [2, 5, 6]. On the basis of satisfactory correlation between $\tau_s(T)$ and $\tau_\delta(T)$ for some types of crystal it was concluded in refs. 2 and 27 that the same point defects determine the dislocation mobility in both dynamic and quasi-static tests at the onset of plastic flow. It should be noted, however, that in some cases rather poor coincidence between the temperature trends $\tau_\delta(T)$ and $\tau_s(T)$ was observed (*e.g.* in LiF [7] and Mo [11]).

Baker [32] proposed a technique for determination of the average dislocation velocity from ADIF experiments. A comparison of acoustic data with those obtained by the etch pit technique showed that the average velocity of dislocations measured by the ADIF method was less sensitive to stress at $\tau<\tau_s$ in comparison with the etch pit velocity [32, 33]. On this basis different

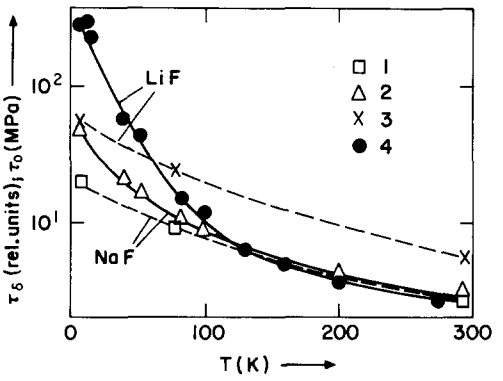

Fig. 1. Temperature dependences of yield stress τ_s (curves 1 and 3) and stress amplitude τ_δ at δ_h=constant (curves 2 and 4) in NaF (curves 1 and 2) and LiF (curves 3 and 4).

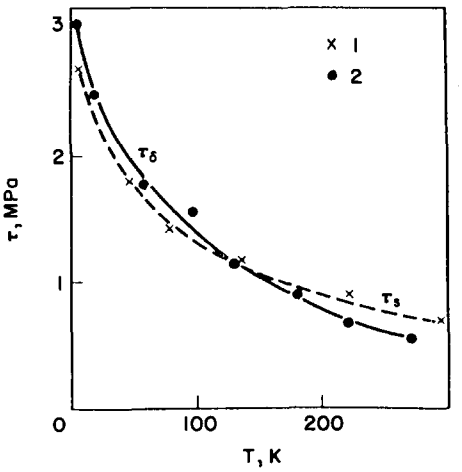

Fig. 2. Temperature dependences of yield stress τ_s (curve 1) and amplitude of vibrational stress τ_δ at δ_h=constant (curve 2) in Al [9].

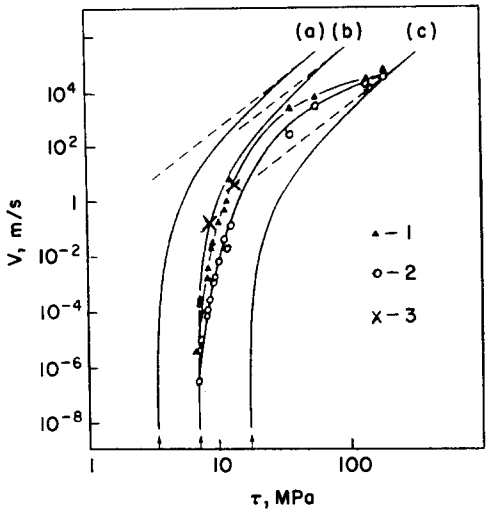

Fig. 3. Average velocity of dislocations *vs.* resolved shear stress $\tau = \tau^* + \tau_i$ in LiF with 0.007% Mg^{2+} (curve a), 0.01% Mg^{2+} (curve b) and 0.03% Mg^{2+} (curve c): —, calculations according to $v = v_0(\tau)^p$, where $\tau = \tau^* + \tau_i$ [2, 28]; – – –, data corresponding to $\tau_i = 0$; curves 1 and 2, etch pit data for edge and screw dislocations obtained by Johnston and Gilman [34]; ×, data from Baker [32] with τ_i from ref. 28.

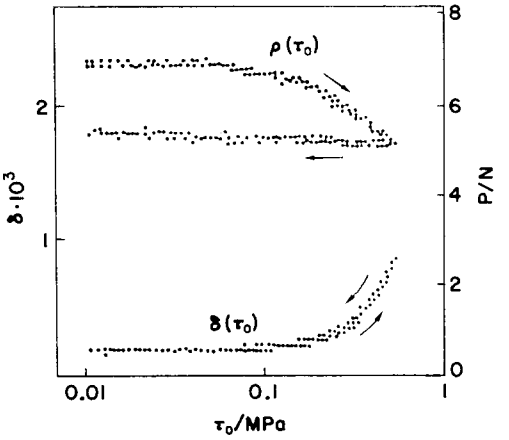

Fig. 4. Decrement δ and load P *vs.* vibrational stress amplitude τ_0 during its gradual increase and decrease at a fixed value of deflection in NaCl.

types of pinning defect in both cases were postulated in ref. 32. In refs. 2 and 28 the average velocity of dislocations, approximately estimated from ADIF and YMD in LiF when the action of an effective stress τ^* and internal stress τ_i was taken into consideration, was also compared with etch pit data. The estimation of the average velocity v in acoustic experiments was similar to that obtained in ref. 32 and based on the equation $v = v_0(\tau^*)^p$, where the effective stress τ^* is the stress amplitude in acoustic experiments. Values of v_0 and p were also calculated from acoustic data. In order to compare this velocity with etch pit data, τ_i was found from the strain rate sensitivity of flow stress. The results of these calculations and estimations of velocity according to Baker's technique using acoustic data for LiF [6] are shown in Fig. 3 *vs.* $\tau = \tau^* + \tau_i$. Etch pit data [34] are shown too. The qualitative agreement in these coordinates is good. This analysis shows that the dislocation loop–point defect interaction is only part of a total spectrum of obstacles overcome by dislocations in quasi-static tests, and probably explains the poor correlation of τ_δ with macroscopic τ_s.

4. Acoustoplastic effect and ADIF

Attempts were made to extend the investigations of interconnection of anelastic strain in acoustic experiments with plastic deformation at yield point. It was known that the additional vibrational stress increases the creep rate [35] or decreases the flow stress during active deformation [36]. Two types of experiment were performed. ADIF was studied during deformation and creep [13–17]. The changes of flow stress due to the acoustoplastic effect and of the acoustic energy damping were investigated simultaneously.

A sharp fall in th flow stress in the stress–strain diagram corresponding to the onset of the acoustoplastic effect at the start of amplitude dependence of δ was observed. The dependences of the deforming load and decrement on the vibrational amplitude in NaCl are shown in Fig. 4. It can be seen that the fall in the deforming load takes place at the same amplitudes when δ begins to increase. A simultaneous rise in the acoustoplastic effect and the amplitude dependence of the internal friction confirms that the same defects can control dislocation mobility in acoustic experiments and during quasi-static deformation. In contrast, there is no such simultaneity in Zn single crystals, when different slip systems operate under ultrasonic and static loads [17], and in polycrystals of aluminium alloy D16 [37]. A detailed discussion of this subject can be found elsewhere [37].

5. Micro- and macroyield stress

Distinctions (in relative units) between $\tau_\delta(T)$ and $\tau_s(T)$ are clearly visible in Fig. 1. These discrepancies were explained by a difference in the conditions of deformation and the possibility of dislocation multiplication during measurements of yield points [2, 27]. However, in the case of LiF [7] the difference between τ_δ and τ_s at low temperatures was so large that it was not possible to speak about any correlation (Fig. 1). Lebedev and Kustov [38] analysed the situation and suggested that $\tau_s(T)$ should be compared with the temperature dependence of τ_ϵ for which the reversible dislocation strain ϵ_d was constant:

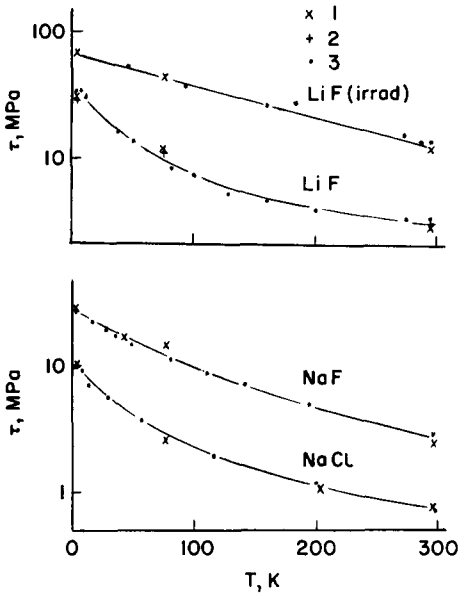

Fig. 5. Temperature dependences of yield stress τ_s (×) and amplitude of vibrational stress τ_ϵ at $\epsilon_d = \delta_h \epsilon = \text{constant}$ (+, ·) for LiF, NaF and NaCl [38, 39].

$$\epsilon_d = \epsilon_0 \Delta E/E = \epsilon_0 \delta_h / r = \text{constant}$$

The $\tau_\epsilon(T)$ dependence in NaF, NaCl and LiF plotted in relative units is shown in Fig. 5 and compared with $\tau_s(T)$. There is a good coincidence. The similarity at low temperatures ($T < 0.3T_m$) has been confirmed not only for the crystals investigated but also for a large variety of crystals where data on τ_s and ADIF were available [10, 11, 38, 39]. Some deviations from this similarity (at 180 K for pure Mo [11] and at 150 K for Al alloys [10]) are connected with the intensive ageing process, confirmed by observed Young's modulus and resistivity recovery at the same temperatures.

Detailed discussion of the physical reasons for the similarity law $\tau_s(T) \approx \tau_\epsilon(T)$ is given elsewhere [39, 40]. Taking into consideration that the string model of the dislocation segment breakaway cannot explain some experimental facts (the shape of the stress–strain loop [18, 30], the absence of any effect of bias stress on ADIF [15, 18, 30]) and the observed coincidence of $\tau_s(T)$ with $\tau_\epsilon(T)$, we have to conclude that thermally activated breakaway of dislocation segments from point defects can contribute only partly to deformation in both ADIF and quasi-static tests.

6. Frequency dependence of anelastic strain and ADIF

The investigations of microplastic reversible dislocation strain at low frequencies were used to clear up the interconnection between the behaviour of material in acoustic and quasi-static tests. Moreover, the direct observations of cyclic stress–reversible anelastic strain dependences under different conditions enabled us to make decisions about the mechanisms controlling the anelastic behaviour of material. In particular, the possibility of studying the frequency dependence of ADIF, YMD and anelastic strain is very important.

An analysis of the shape of stress–anelastic strain hysteresis loops and of the influence of static stress on cyclic anelastic strain resulted in the conclusion in ref. 18 that the anelastic behaviour of crystals should be explained within a framework of "unlocalized friction" models rather than the "breakaway" models in both the infra- and ultrasonic ranges. Further investigation of the hysteresis loop during cyclic and transient loading of the samples shows that a quasi-static hysteresis loop of non-zero area exists inside the dynamic steady state hysteresis loop [20]. It seems reasonable to propose that the steady state hysteresis loop at non-zero frequencies is formed by two stress components: the first forms the quasi-static loop, and the second provides the deformation with non-zero strain rate $\dot{\epsilon}_{an}$. These components form two parts of the ADIF.

The area of the quasi-static hysteresis loop corresponds to the hysteretic or athermal part of the dissipated energy. The area between the steady state and quasi-static hysteresis loops corresponds to the part of the ADIF caused by thermally activated overcoming of short-range obstacles by moving dislocations. The dependences of the effective stress τ^* on strain rate $\dot{\epsilon}_{an}$, determined on the basis of the hysteresis loops at different frequencies, and the macroscopic effective stress as a function of $\dot{\epsilon}$, determined by the strain rate sensitivity of the flow stress, are given by the same power function $\tau^* = k_1 \dot{\epsilon}_{an}^m$. By analogy with macroscopic deformation the second component of stress can be considered identical to the internal stress τ_i. Then the quasi-static hysteresis loop can be ascribed to the athermal internal stress field hysteresis. Some insights into the nature of internal stress field hysteresis are given in ref. 22. The anelastic strain can also be linked to the internal stress changes by a power function [20]: $\epsilon_{an} = k_2 \tau_i^n$. This gives the possibility of forming a differential equation for the loading part of the hysteresis loop: $\epsilon_{an}(t) = k_2\{\tau(t) - k_1[\dot{\epsilon}_{an}(t)]^m\}^n$. The unloading part of the hysteresis loop is symmetrical. This equation was solved numerically for different amplitudes and frequencies [21].

The amplitude dependences of the decrement, YMD and the contribution of the quasi-static athermal component of damping are shown in Fig. 6 for LiF and NaCl. The experimental and calculated data are in good agreement. Some discrepancy in LiF can be explained by the amplitude hysteresis and time dependences of δ_h and $\Delta E/E$. These effects are not taken into account. The results of calculation of the frequency

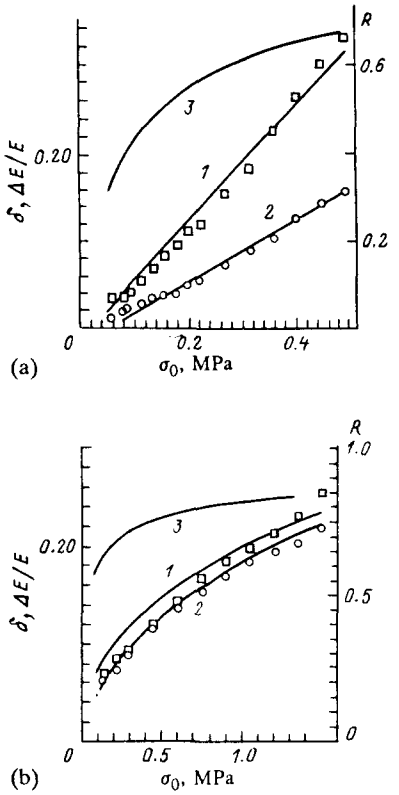

Fig. 6. Amplitude dependences of the decrement (curves 1), YMD (curves 2) and the fraction of quasi-static athermal damping (curves 3) in (a) LiF and (b) NaCl at a frequency of 0.5 Hz: —, results of calculations [21].

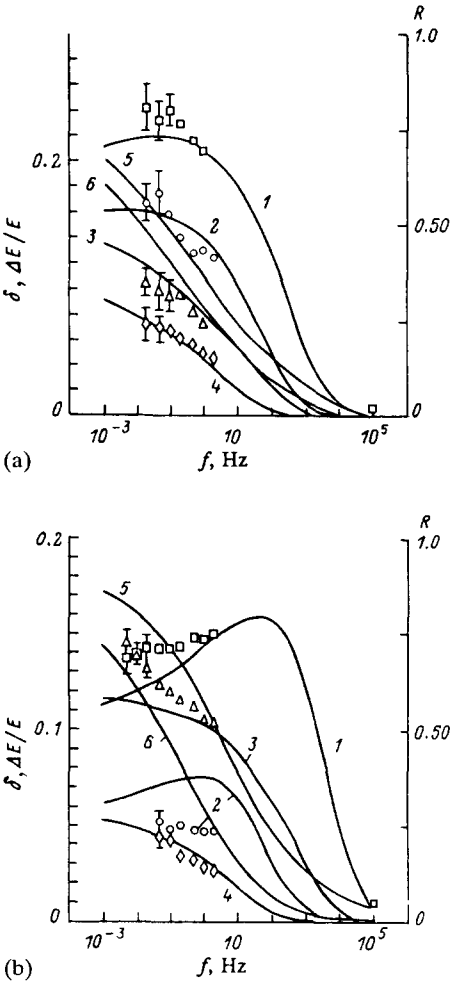

Fig. 7. Calculated and experimental dependences of the decrement (curves 1 and 2), YMD (curves 3 and 4) and the fraction of quasi-static athermal damping (curves 5 and 6) on frequency [21]: (a) NaCl crystal at amplitudes of 0.43 MPa (curves 1, 3 and 5) and 0.29 MPa (curves 2, 4 and 6); (b) LiF crystal at amplitudes of 1.6 MPa (curves 1, 3 and 5) and 0.4 MPa (curves 2, 4 and 6).

dependences of δ_h and $\Delta E/E$ of NaCl and LiF for frequencies of 10^{-3}–10^5 Hz are shown in Fig. 7. Experimental data for δ_h in the infrasonic range and at 100 kHz (shown by points) are in good agreement with the calculated dependences. The monotonic fall of $\Delta E/E$ with increasing frequency and more complicated behaviour of δ_h can be seen. A frequency maximum can be observed, whose position depends on the strain amplitude. The calculated dependences of the quasi-static athermal and thermally activated components of ADIF are shown in Fig. 8. The thermally activated part has a maximum as predicted by theory [23]. The athermal part decreases with increasing frequency. The frequency dependence of the athermal component of δ_h is caused by redistribution of the applied stresses between effective and internal stresses with change of frequency.

The proposed description of ADIF is attributed in ref. 21 to a combination of the processes of cyclic strain hardening, manifested by a hysteresis of the internal stress field, with thermally activated overcoming of short-range obstacles by dislocations under the influence of the effective stress component. Furthermore, the dependences of effective stress on strain rate are similar for ADIF tests and macroscopic deformation. Figures 6 and 7 show that the contribution of the quasi-static athermal component of ADIF decreases with decreasing stress amplitude and increasing frequency. It was concluded in ref. 21 that this is evidence of a certain sequence of activation of different ADIF mechanisms. The lower is the anelastic strain amplitude, the higher is the contribution of dislocation interactions with short-range obstacles. The increase in anelastic strain results in the increase of internal stress field changes or in the contribution of a larger-scale process of interaction of dislocations.

The values of $\Delta E/E$ calculated in the ultrasonic range are more than an order of magnitude lower than the experimental values. This discrepancy is explained in ref. 21 by the action of an athermal mechanism linked to the effective stress component, *i.e.* to force or athermal

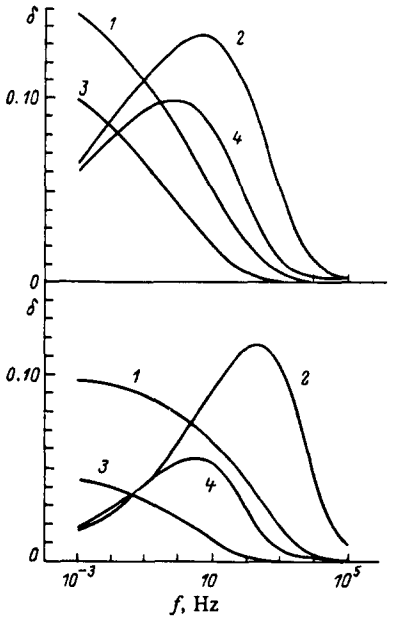

Fig. 8. Calculated frequency dependences of the force component (curves 1 and 3) and thermally activated component (curves 2 and 4) of damping [21]: (a) NaCl crystal at amplitudes of 0.43 MPa (curves 1 and 2) and 0.29 MPa (curves 3 and 4); (b) LiF crystal at amplitudes of 1.6 MPa (curves 1 and 2) and 0.4 MPa (curves 3 and 4).

overcoming of short-range obstacles at high values of the effective stress rate $\dot{\tau}^*$ in the ultrasonic range. This mechanism, which has not been taken into consideration yet, is expected in ref. 21 to explain the higher mobility of dislocations in the ultrasonic range than in the infrasonic range and quasi-static tests.

7. Conclusions

The experimental study of the amplitude, temperature and frequency dependences of the ADIF and YMD for a variety of crystals was carried out. The similarity of the temperature dependences of vibrational stress at constant reversible dislocation strain and of the yield stress and simultaneous rise of the acoustoplastic effect and amplitude dependence of damping show that under certain circumstances the same obstacles control the deformation in acoustic and quasi-static tests. It is concluded that existing microscopic dislocation breakaway theories cannot give a reliable explanation for the observed phenomena.

From the phenomenological point of view different mechanisms of plasticity – reversible strain hardening, or thermally activated or athermal overcoming of short-range obstacles – can contribute to ADIF depending on the frequency, amplitude and temperature ranges.

References

1 J. Marx, *Rev. Sci. Instrum., 22* (1951) 503.
2 S.P. Nikanorov and B.K. Kardashev, *Elasticity and Dislocation Anelasticity of Crystals,* Nauka, Moscow, 1985 (in Russian).
3 B.K. Kardashev, S.P. Nikanorov and O.A. Voinova, *Fiz. Tverd.Tela, 16* (1974) 1068.
4 B.K. Kardashev, S.P. Nikanorov and O.A. Voinova, *Phys. Status Solidi A, 12* (1972) 375.
5 O.A. Voinova, B.K. Kardashev and S.P. Nikanorov, *Fiz. Tverd. Tela, 22* (1980) 1052.
6 O.A. Voinova, B.K. Kardashev and S.P. Nikanorov, *Fiz. Tverd. Tela, 23* (1981) 2933.
7 K. Khaidarov, A. Shalpikov, B.K. Kardashev, A.B. Lebedev and S.P. Nikanorov, *Izv. Akad. Nauk Kirg. SSR,* (1) (1980) 23.
8 B.K. Kardashev, S.B. Kustov, A.B. Lebedev, G.V. Berezhkova, P.P. Perstnev, F. Appel and U. Messerschmidt, *Phys. Status Solidi A, 91* (1985) 79.
9 V.I. Ivanov, B.K. Kardashev and S.P. Nikanorov, *Phys. Status Solidi A, 65* (1981) 335.
10 A.B. Lebedev, *Fiz. Tverd. Tela, 34* (1992) 1889.
11 A.B. Lebedev, B.K. Kardashev, U. Hoffman, H.J. Kaufmann and D. Schulze, *Cryst. Res. Technol., 24* (1989) 1143.
12 S.P. Nikanorov, A.D. Romanov and E.A. Zinman, *Fiz. Tverd. Tela, 16* (1974) 2984.
13 A.B. Lebedev, S.B. Kustov and B.K. Kardashev, *Fiz. Tverd. Tela, 24* (1982) 3169.
14 A.B. Lebedev, S.B. Kustov and B.K. Kardashev, *Fiz. Tverd. Tela, 25* (1983) 890.
15 A.B. Lebedev, S.B. Kustov and B.K. Kardashev, *Fiz. Tverd. Tela, 31* (1989) 62.
16 A.B. Lebedev, S.B. Kustov and B.K. Kardashev, *Fiz. Tverd. Tela, 29* (1987) 3563.
17 A.B. Lebedev, Yu.A. Burenkov and T.I. Golubenko, *Fiz. Tverd. Tela, 35* (1993) 420.
18 S.B. Kustov, S.N. Golyandin and B.K. Kardashev, *Sov. Phys. – Solid State, 30* (1988) 1248.
19 S.B. Kustov, S.N. Golyandin and B.K. Kardashev, *Sov. Phys. – Solid State, 31* (1989) 326.
20 S.N. Golyandin and S.B. Kustov, *Sov. Phys. – Solid State, 34* (1992) 2031.
21 S.N. Golyandin and S.B. Kustov, *Sov. Phys – Solid State, 34* (1992) 2035.
22 S.N. Golyandin and S.B. Kustov, *J. Alloys Comp.,* (this conference, in print).
23 K. Lucke, A.V. Granato and L.J. Teutonico, *J. Appl. Phys., 39* (1968) 5181.
24 V.L. Indenbom and V.M. Chernov, *Phys. Status Solidi A, 14* (1972) 347.
25 R.B. Schwarz and A.V. Granato, *Phys. Rev. Lett., 34* (1975) 1174.
26 M. Gabbay, A. Vincent and G. Fantozzi, *Phys. Status Solidi A, 100* (1987) 121.
27 B.K. Kardashev, *Fiz. Tverd. Tela, 19* (1977) 2490.
28 B.K. Kardashev and S.P. Nikanorov, *Fiz. Tverd. Tela, 27* (1985) 3057.
29 P.P. Pal-Val, V. Ya. Platkov and V.I. Starzev, *J. Phys. (Paris), Colloq. C5, Suppl., 42* (1981) 259.
30 V.I. Ivanov, B.K. Kardashev, S.B. Kustov, A.B. Lebedev and S.P. Nikanorov, in T.S. Ke (ed.), *Proc. 9th Int. Conf. on Internal Friction and Ultrasonic Attenuation in Solids, Beijing, July 1989,* Pergamon, Oxford, 1990, p.159.
31 R.B. Schwarz, R.D. Isaac and A.V. Granato, *Phys. Rev. Lett., 38* (1977) 554.

32 G.S. Baker, *J. Appl. Phys., 33* (1962) 1730.
33 V.Ya. Platkov, V.P. Efimenko and V.I. Starzev, *Fiz. Tverd. Tela, 9* (1967) 2799.
34 W.G. Johnston and J.J. Gilman, *J. Appl. Phys., 30* (1959) 129.
35 L. Archbutt, *Trans. Faraday Soc., 17* (1921) 22.
36 F. Blacha and B. Langenecker, *Naturwissenschaften, 42* (1955) 556.
37 A.B. Lebedev, *Fiz. Tverd. Tela, 35* (1993) 2305.
38 A.B. Lebedev and S.B. Kustov, *Fiz. Tverd. Tela, 29* (1987) 915.
39 A.B. Lebedev and S.B. Kustov, *Phys. Status Solidi A, 116* (1989) 645.
40 A.B. Lebedev, *J. Alloys Comp.*, (this conference, in print).